Amino Acids (2015) 47:135–146
DOI 10.1007/s00726-014-1848-2

ORIGINAL ARTICLE

Employing in vitro analysis to test the potency of methylglyoxal in inducing the formation of amyloid-like aggregates of caprine brain cystatin

Waseem Feeroze Bhat · Sheraz Ahmad Bhat · Peerzada Shariq Shaheen Khaki · Bilqees Bano

Received: 22 August 2014 / Accepted: 29 September 2014 / Published online: 21 October 2014

Abstract Thiol protease inhibitors (cystatins) are implicated in various disease states from cancer to neurodegenerative conditions and immune responses. Cystatins have high amyloidogenic propensity and they are prone to form fibrillar aggregates leading to amyloidosis. Particularly challenging examples of such disorders occur in type 2 diabetes, Alzheimer's and Parkinson's diseases. The aim of the present study is to find an interaction between the compound methylglyoxal (MG) which is particularly elevated in type 2 diabetes with caprine brain cystatin (CBC). Results have shown that elevated concentration of MG forms amyloid aggregates of CBC. This was achieved by allowing slow growth in a solution containing moderate to high concentrations of MG. When analysed with microscopy, the protein aggregate present in the sample after incubation consisted of extended filaments with ordered structures. This fibrillar material possesses extensive β-sheet structure as revealed by far-UV CD and IR spectroscopy. Furthermore, the fibrils exhibit increased Thioflavin T fluorescence.

Keywords Caprine brain cystatin · Methylglyoxal · Amyloid · Fluorescence · β-Sheet · Diabetes

Abbreviations

MG	Methylglyoxal
CBC	Caprine brain cystatin
AGEs	Advanced glycation end products
AD	Alzheimer disease
PD	Parkinson's disease
mM	Millimolar

Introduction

Brain is a surprisingly active tissue in terms of glucose metabolism; almost all the energy supplied to maintain its vital functions are derived from glucose oxidation. Because very little glycogen is stored in the brain, the high energy requirements of the central nervous system must be met by external sources of glucose. Thus, the brain is highly vulnerable to hypoglycaemia and may suffer irreversible damage after hypoglycaemic events (Marks 1992). However, epidemiological data have shown that hyperglycaemia was associated with higher risks of strokes and that ischemic cerebral injury was, at least partly, attributed to hyperglycaemia as well (Asplund et al. 1980; Riddle and Hart 1982; Pulsinelli et al. 1983). Hyperglycaemia is associated with diabetes; in fact, chronic hyperglycaemia is the defining characteristic of the disease. Intermittent hyperglycaemia may be present in prediabetic states. Acute episodes of hyperglycaemia without an obvious cause may indicate developing diabetes or a predisposition to the disorder. The first disease state where evidences emerged for increased formation of methylglyoxal (MG)[1] and ketone bodies is in fact diabetes. It is noteworthy to mention that in a diabetic patient the concentration of ketone bodies can exceed up to 25 mM (Laffel 1999; Stephens et al. 1971) but in normal individuals their concentration is less than 0.5 mM (Candiloros et al. 1995). Apart from elevated blood glucose levels, both glucose and ketone bodies are the influential compounds for the production of MG. The highly

Electronic supplementary material The online version of this article (doi:10.1007/s00726-014-1848-2) contains supplementary material, which is available to authorized users.

W. F. Bhat · S. A. Bhat · P. S. S. Khaki · B. Bano (✉)
Department of Biochemistry, Faculty of Life Sciences, Aligarh Muslim University, Aligarh 202002, UP, India
e-mail: bilqeesbano99@gmail.com

consequential relationship that was observed between acetol (ketone body) and MG suggests that MG is produced directly from acetol by oxidative mechanisms (Thornalley 1996). The relationship between MG and acetol with a linear regression analysis was found to be highly significant (Beisswenger et al. 2005), with a similar highly significant relationship between Beta hydroxybutyrate, acetol and acetone. Plasma MG levels in healthy human subjects are 1–4 μM (Wang et al. 2007; Thornalley et al. 1989). However, the physiological concentration of MG in normal rats is between 0.5 and 10 μM (Wang et al. 2004). In patients with type 2 diabetes, plasma MG levels are twofold to fourfold elevated (McLellan et al. 1994). This increase in MG concentration leads to modification of various proteins in the body. Being up to 40,000 times more chemically reactive than glucose, it has multiple cytotoxic effects (Fig. 1). These include inhibition of cell growth, apoptosis, mutagenic effects, inhibition of enzymatic activity, production of protein cross-linking and fragmentation, and serving as an important precursor for advanced glycation end product (AGE) formation. Hotspot protein targets of methylglyoxal that suffer functional impairment—the dicarbonyl proteome—likely play a key role in the mechanisms underlying the development of vascular complications in diabetes.

In diabetes, hyperglycaemia triggers enhanced production of methylglyoxal, one consequence of which is the rapid modification of proteins and other substrates to generate what are called advanced glycation end products, or AGEs (Shinohara et al. 1998). The in vitro experiments suggest that glycoxidation (oxidation of the Amadori or Heyn's product) is the predominant chemical pathway in the formation of AGE-derived cross-links on β-amyloid peptide. It is reported that in vitro glycation of tau protein resulted in paired helical filaments (Ledesma et al. 1994). Incubation of β-amyloid peptide with sugars causes the formation of high-molecular-mass oligomers. These oligomers and aggregates are able to interact and associate with cell membranes because of their exposed hydrophobic surfaces and can generate toxicity and impairment of cellular function (Stefani and Dobson 2003). The exact cause underlying protein aggregation and misfolding remains unknown presenting a seemingly insurmountable challenge to delineate the conditions(protein sequence, pH, temperature, presence of metals/toxicants) existing in vivo forcing the proteins to aggregate and collect as amyloid deposits leading to incurable and often debilitating consequences. Under various conditions, many proteins can aggregate to regular arrays of β-sheet-rich filaments or fibres of indefinite length, often coiled together in higher order structures. The ability to fibrillate is independent of the original native structure of the protein, whose amino acid sequence primarily appears to play a role in terms of filament arrangement, fibrillation kinetics and overall yield and stability of

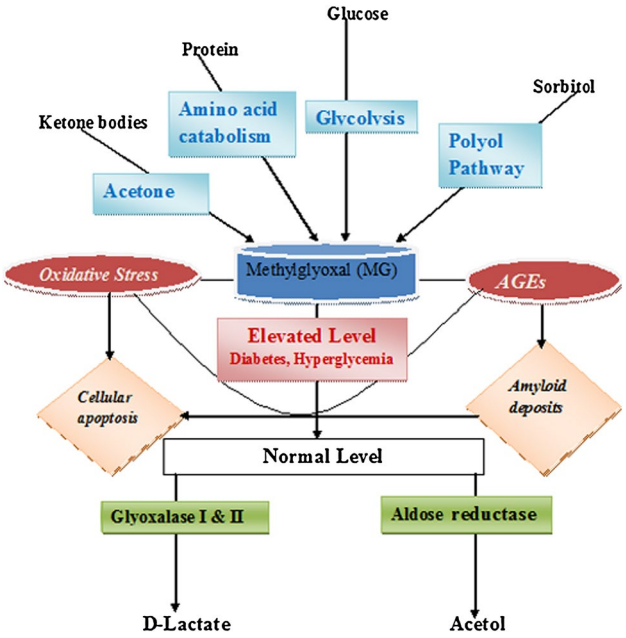

Fig. 1 Schematic diagram showing the formation of MG from different sources, degradation of MG in normal levels and fate of MG during elevated levels (normally in hyperglycaemia and diabetes)

the fibrils. It typically occurs under conditions that stabilise partially folded or unfolded states (Holm et al. 2007).

Fibril formation is, thus, generic property of proteins (Fandrich et al. 2001). Fibrillation generally starts from an intermediate state, either partially unfolded or partially folded, molten globule or native-like intermediate (Rochet and Lansbury 2000). In case of globular proteins such as cystatin C partial unfolding (Ekiel and Abhrahamson 1996), and for α-synuclein, unfolded polypeptides (Uversky et al. 2001) are the initiation points for fibrillation. In vitro variation of solvent conditions by changing pH or adding organic solvents can lead to partial unfolding and subsequent protein fibril formation. With unfolded polypeptides, partial folding can be obtained by lowering pH or by heating. In vivo, partial unfolding may happen as a consequence of lowered protein stability due to mutation, local change in pH of membranes, oxidative and heat stress, where as partial folding may happen on exposure to environmental hydrophobic substances, such as chemicals and pesticides (Zervonik et al. 2006).

Cystatins, a family of structurally related cysteine proteinase inhibitors, have proved to be a useful model system to study amyloidogenesis (Skerget et al. 2009). Cystatins are crucial for proper brain functioning. It has been investigated that lysosomal proteinase (cathepsins) and their endogenous inhibitors (cystatins) have been closely associated with senile plaques, cerebrovascular amyloid deposits and neurofibrillary tangles in Alzheimer disease (AD) and Parkinson's disease (PD) (Ii et al. 1993; Bernstein et al.

1996). The over expression of human cystatin C in brains of APP-transgenic mice reduces cerebral amyloid-β deposition and that cystatin C binds amyloid-β and inhibits its fibril formation (Stephan et al. 2007), However, results have shown that cystatin C caused the disappearance of the fibrils and appearance of amorphous aggregates (Sastre et al. 2004). Most importantly, the occurrence of cystatin C in Aβ amyloid deposits may result from cystatin C binding to the precursor protein prior to Aβ generation, or alternatively, cystatin C may bind to Aβ prior to its secretion, or following Aβ deposition in the brain.

Cystatins are prone to form amyloid (Skerget et al. 2009). Cystatin C L68Q variant is an amyloid fibril-forming protein with a high tendency to dimerize. It forms self-aggregates with massive amyloid deposits in the brain arteries of young adults, leading to lethal cerebral haemorrhage (Mussap and Plebani 2004). The fibril formation is also known to occur in chicken cystatin, Latexin stefin A and stefin B under in vitro conditions (Zerovnik et al. 2007; Turk et al. 2008). In the present study, the interaction of CBC with MG has been investigated and it was found that maximum unfolded state has been achieved on day 9 of incubation with different concentrations of MG, and the aggregated state was obtained on day 14. Using fluorescence studies, it was found that the intermediate state which is possibly a misfolded state sets the path for CBC aggregation.

Materials and methods

Materials

Methyl Glyoxal (MG), Thioflavin T, and ANS (8-anilino-1-naphthalenesulfonic acid) were procured from Sigma, Aldrich USA. The solutions were prepared in 50 mM phosphate buffer of pH 7.4. Salts were purchased from Merck (India). The protein concentration was determined spectrophotometrically. All other reagents were of analytical grade, and double distilled water was used throughout.

Purification of brain cystatin

The purification of cystatin was achieved by modification of the method reported earlier by Amin et al. (2011). Caprine brain whole mass (150 g) was brought fresh from slaughter house in an ice bucket. It was thoroughly washed with water, thin membrane and nerves were removed by forceps, and the whole brain tissue was homogenised in 50 mM sodium phosphate buffer (300 mL) of pH 7.5 containing 0.15 M NaCl, 3 mM EDTA, and 2 % *n*-butanol. After centrifugation at 11,000 rpm for 15 min at 4 °C, residue was discarded and the supernatant was further processed. The

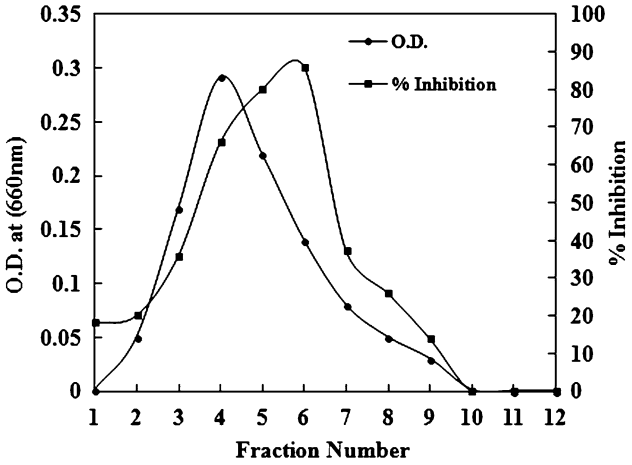

Fig. 2 Gel filtration of CBC on a column of Sephacryl S-100 HR. The precipitate obtained from 40 to 60 % ammonium sulphate saturation was subjected to gel filtration at a flow rate of 20 ml/h. Fractions of 5 ml were collected and monitored by inhibition of caseinolytic activity of papain. Fractions *4*, *5*, *6*, were pooled for further studies

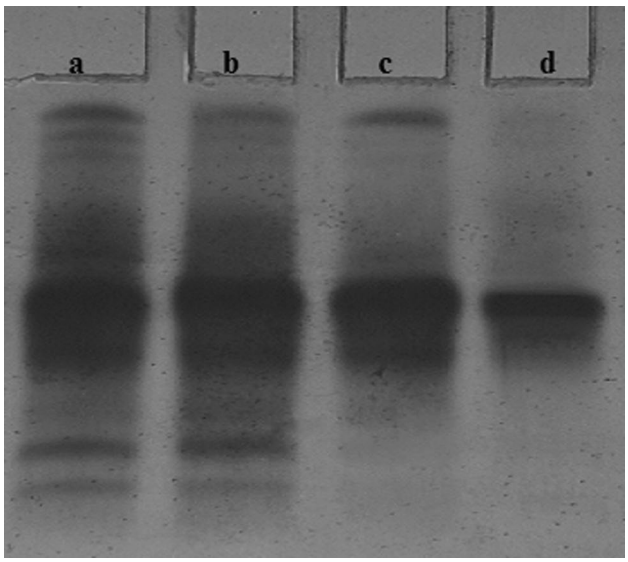

Fig. 3 Gel electrophoresis of CBC during various stages of purification. Electrophoresis was performed on 7.5 % gel. *Lane a* contained 60 µg caprine brain homogenate, *lane b* contained 60 µg homogenate after alkaline treatment, *lane c* is 60 µg dialyzed fraction after ammonium sulphate fractionation, *lane d* is 60 µg brain cystatin after Sephacryl S-100 HR gel filtration

procedure involved a combination of alkaline treatment (pH 11.0), ammonium sulphate precipitation (40–60 %) and gel filtration chromatography on sephacryl S-100 HR with 20.46 % yield and 312-fold purification. A single protein peak with papain inhibitory activity (Fig. 2) was obtained corresponding to the caprine brain cystatin (CBC). Papain inhibitory fractions of peak were pooled, concentrated, and

checked for purity. Five millilitre fractions were collected and assayed for protein and cystatin activity. Homogeneity of the preparation was investigated by 7.5 % PAGE (Fig. 3). The molecular mass of the inhibitor as determined by its electrophoretic and gel filtration behaviour was found to be ~44 kDa (see Supplementary Information).

Interaction of CBC with MG

To investigate the effect of the MG on the structural integrity of CBC, 50 μM CBC samples were incubated with 150 mM sodium chloride, 0.1 mM sodium azide and sodium phosphate buffer (50 mM, pH 7.4) in the presence of 1–10 mM MG in capped vials under sterile conditions for a period of 14 days (2 weeks) at 37 °C. To eliminate possible contaminations, all dishes were autoclaved prior to use and all solutions were filtered. Aliquots were taken day wise to carry out spectroscopic analysis.

Assay of proteinase inhibitor activity

The inhibitory activity of CBC was assessed by its ability to inhibit the caseinolytic activity of Papain by the method of Kunitz (1947). Papain was incubated with various amounts of inhibitor in 1 ml of sodium phosphate buffer, pH 7.5 containing 0.14 M cysteine and 0.047 M EDTA at 37 °C for 40 min. One millilitre of 2 % casein was added and the mixture was further incubated for 30 min. The reaction was stopped by adding 10 % TCA, after centrifugation at 2,500 rpm for 10 min. Protein concentration was estimated in the supernatant by the method of Lowry et al. (1951).

Intrinsic fluorescence measurements

The fluorescence intensity of tryptophan residue was measured in a Shimadzu RF-5301 spectrofluorophotometer (Tokyo, Japan) with both emission and excitation slits equal to 5 nm. Protein concentration used was 0.2 mg/ml. The emission spectra were recorded over a wavelength range of 300–500 nm. The excitation of protein samples was at 285 nm.

ANS fluorescence measurements

8-Anilino-1-naphthalenesulfonic acid (ANS) is a compound that is used for probing the available hydrophobic domains in proteins. Its binding was measured by exciting the sample at 385 nm and emission recorded using Shimadzu Rf-5301 spectrofluorophotometer (Tokyo, japan) from 400 to 600 nm. Typically, ANS concentration was taken 100 molar excess of protein concentration while protein concentration was taken 2.5 μM (Bhat et al. 2014).

Thioflavin T fluorescence assay

Thioflavin T (ThT) dye being indicative for amyloid/aggregate testimonial (Tokunaga et al. 2013). Fluorescence was measured to monitor amyloid aggregation of CBC. Typically, 40 μL of protein aggregate sample was diluted using a phosphate buffer (50 mM, pH 7.4) containing ThT to a final concentration of 10 μM ThT in pH 7.4 at room temperature (Kumar and Udgaonkar 2009). The following parameters were adjusted for monitoring ThT fluorescence intensity during experiments: ThT fluorescence emission was measured with excitation at 450 nm and recording the spectrum between 465 and 565 nm with 5 nm slits using a Shimadzu RF 5301 spectrofluorophotometer (Tokyo, Japan). Emission spectra between 465 and 565 nm were recorded upon excitation at 450 nm.

Circular dichroism (CD) measurements

Circular dichroism (CD) measurements were carried out on a JASCO spectropolarimeter (J-816). The instrument was calibrated with D- 10-camphorsulfonic acid. All the CD measurements were carried out at 25 °C with a thermostatically controlled cell holder attached to a Neslab RTE-110 water bath with an accuracy of ±0.1 °C. Spectra were collected with a scan speed of 100 nm/min and a response time of 2 s. Each spectrum was average of three scans. Far-UV CD spectra measurements were carried at a protein concentration of 0.2 mg/ml in the range of 200–250 nm in a cell of 0.1 cm path length. All spectra were smoothed by the Savitzky–Golay method with 25 convolution width. Results of the CD measurements were converted to $[\theta]_\lambda$, the mean residue ellipticity (deg cm^2 mol^{-1}) at wavelength λ (nm) using the Eq. (1).

$$[\theta]_\lambda = \frac{\theta_\lambda M_0}{10 \times c \times l} \quad (1)$$

where $[\theta]_\lambda$ is ellipticity (milli degree) at λ, M_0 is the mean residue weight, c is protein concentration (mg/ml), and l is path length (cm). The amount of secondary structure was obtained using K2D2 online software.

FTIR spectral studies

FTIR spectra were recorded at room temperature using Spectrum Two FTIR spectrometer (Perkin Elmer) equipped with deuterium triglycine sulphate (DTGS) detector. CBC samples incubated with and without MG were placed between CaF_2 windows separated with a spacer. Each spectrum represents the average of 256 scans recorded in the region 4,000–400 cm^{-1} keeping 4 cm^{-1} resolution. For all spectra, the area between 1,580 and 1,710 cm^{-1} has been normalised to unity.

Transmission electron microscopy (TEM)

Transmission electron micrographs were collected on TECNAI G2, FEI Company (Holland) transmission electron microscope operating at an accelerating voltage of 200 kV. Fibrillar-like aggregate structure of CBC was assessed by applying 10 µl of protein sample on a carbon-coated copper grid and left to adsorb for 1 min. After excess fluids were removed from the grid surface, the grid was washed with distilled water and stained with 0.3 % aqueous uranyl acetate. Excess stain was removed and the samples were dried at room temperature. Images were captured with AMT digital camera system.

Results

Prior to embarking on aggregation studies, the conformational and size changes of CBC were investigated by fluorescence and CD spectroscopy during different stages of incubation period, while days 13 and 14 has shown ~maximum change, which has been taken for final effect of MG on CBC.

CBC activity profile

To investigate whether MG induced a change in CBC enzyme activity, aliquots at different incubation time intervals were withdrawn for Thiol proteinase activity. CBC was found to lose its Papain inhibitory activity by incubation with increasing concentration of MG. The results are summarised in Table 1. CBC modified with 10 mM MG lost as much as 98 % of its antiproteolytic activity and CBC+5 mM MG also lost ~90 % of its activity within 12 days of incubation, while after two weeks of incubation none of the above two samples showed activity. However, CBC modified with 1 mM MG retained ~30 % its activity after the 14 days of incubation. This decrease in the activity of the MG-treated CBC suggests that the enzyme has started to lose its native structure in which it was biologically active and the enzyme might have deviated from its original structure and attained an unfolded state, which finally could lead to aggregation of CBC.

Fluorescence studies

To investigate whether MG induced a change in the tertiary structure of CBC, aliquots at different incubation time intervals were withdrawn and intrinsic protein fluorescence was measured. However, results are presented only at which perceivable peak changes were observed. Intrinsic fluorescence measurement is an interesting method to observe unfolded or molten globule structure of proteins.

Table 1 Effect of MG on antiproteolytic activity of CBC

Time of incubation (days)	%CBC activity		
	CBC+1 mM MG	CBC+5 mM MG	CBC+10 mM MG
0	99.23 ± 5.1* (−0.77)	98.36 ± 5.8* (−1.64)	98.23 ± 4.0* (−1.77)
5	68.26 ± 2.3* (−31.74)	49.23 ± 0.86* (−50.77)	37.32 ± 0.82* (−62.68)
10	39.50 ± 1.2* (−60.50)	19.53 ± 0.58* (−80.47)	11.25 ± 0.07* (−88.75)
12	34.30 ± 0.57* (−65.70)	10.37 ± 0.67* (−89.63)	1.17 ± 0.03* (−98.83)
14	26.57 ± 0.34* (−73.43)	ND	ND

The activity of native CBC is taken to be 100. Results are mean ± SEM for three separate experiments; values in parentheses represent percent change from control

ND none detected

* Significantly different from native CBC (control) at $p < 0.05$ by one-way ANOVA

Trp fluorescence spectra of the native CBC and the modified CBC by MG exposed for various concentrations are shown in (Fig. 4a). It should be noted that the wavelength of excitation was 295 nm. The emission intensity of the modified CBC by MG decreases with an increase in the concentration of MG. At 1 mM MG, negligible change was observed which increased rapidly at 5 mM MG reaching maximum decline at 10 mM concentration. The time course of the change in the fluorescence intensity is shown in (Fig. 4b). It can also be seen in this figure that 9 days of incubation caused the most decrease in the fluorescence intensity.

The reduction in Tryptophan fluorescence intensity of modified CBC was observed because of Trp transition to polar solvent, so the tertiary structure of modified CBC was changed during the time of incubation compared to that of the native CBC. This short term incubation of CBC with increasing MG concentration caused abrupt decrease in Trp fluorescence suggesting that conformational change accompanied to CBC via MG. A decrease in intrinsic fluorescence intensity caused by tryptophan was previously reported (Coussons et al. 1997). Their experiments also revealed a strong decrease in intrinsic protein fluorescence with increasing sugar concentrations. Contrarily, they did not detect modification of tryptophan in amino acid analysis even after 56 days of incubation with 0.5 M concentration. Therefore, the decrease in tryptophan fluorescence should be due to conformational changes in the protein.

Figure 5 shows the ANS emission spectra of the native and modified CBC with MG incubated for 14 days. It is

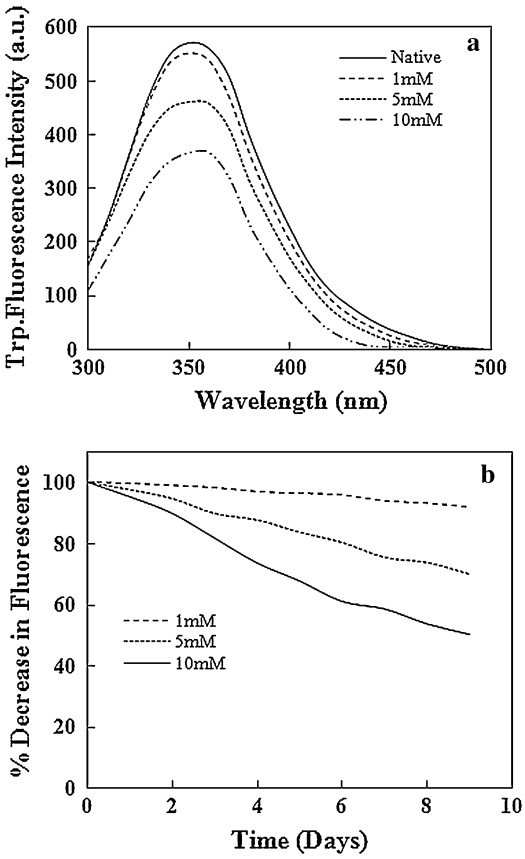

Fig. 4 **a** Fluorescence emission spectra of native and modified CBC by MG with different concentrations, in sodium phosphate buffer (50 mM, pH 7.4), 1 mM EDTA and 0.1 mM sodium azide, incubated at 37 °C. Different *graph curves* show the order of reduction in fluorescence intensity. The emission spectra were taken from 300 to 500 nm; samples were excited at 285 nm. **b** Percent change in fluorescence taking the value of sample incubated without MG as 100 (control)

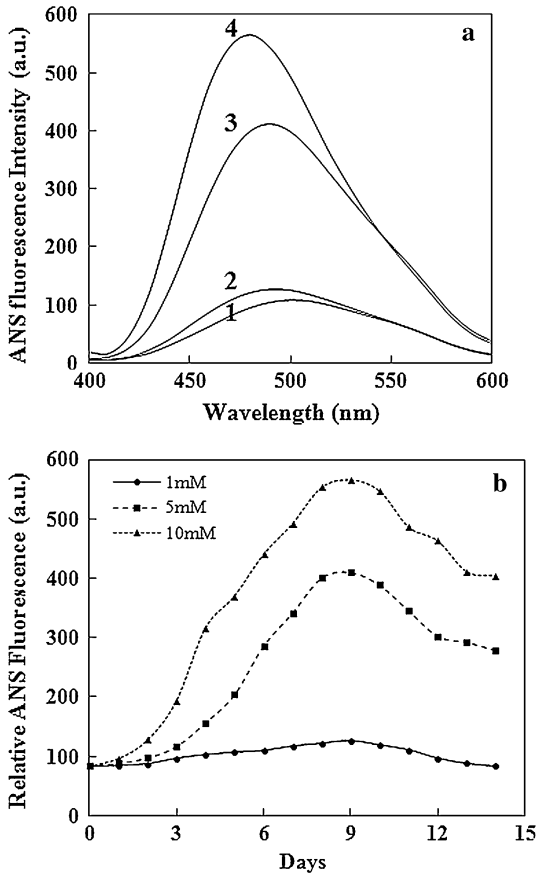

Fig. 5 **a** ANS fluorescence emission spectra of the native CBC (*curve 1*), 1 mM MG+CBC (*curve 2*), 5 mM MG+CBC (*curve 3*) and 10 mM MG+CBC incubated (*curve 4*). **b** Relative ANS fluorescence pattern of CBC incubated with 1, 5 and 10 mM MG from days 0 to 14. Samples were excited at 385 nm and the emission spectra were taken from 400 to 600 nm. The protein concentration was 2.5 μM with a path length of 1 cm

seen in this figure that the fluorescence intensity increases with an increase in the time of incubation. However, this increase is highest for 9 days of incubation, as aggregated (unfolded) species are often present in very low concentrations and may exhibit a short life span characterising the intermediate states involved in the passage from the folded to the unfolded state or vice versa (Carrotta et al. 2001). Extrinsic fluorescent dyes (ANS, Bis-ANS) can provide information about unfolding processes, and can be particularly valuable to evidence the presence or absence of molten globule intermediates. The enhancement of ANS fluorescence intensity is due to the increments of solvent accessibility to its hydrophobic surface areas. The beauty of ANS or Bis-ANS lies in its attachment with proteins via both ionic as well as hydrophobic interactions in an oriented manner, as partially folded intermediate of protein possesses hydrophobic regions adjacent to polar amino acids accessible to both kinds of interactions. On the other hand, completely denatured or completely aggregated protein lacks both charged and hydrophobic regions in an integral manner. It is reported that molten globule intermediates of carbonic anhydrase B and α-lactalbumins show strong affinity to ANS via solvated hydrophobic core (Semisotnov et al. 1987). The highest hydrophobicity was observed for modified CBC incubated with 10 mM MG. This suggested that amyloid-like aggregates of CBC induced by MG passes through a state similar to molten globular intermediate or partially folded state. In addition to an intensity increase, a blue shift in ANS fluorescence emission maximum demonstrated the exposure of hydrophobic surfaces on molten globules CBC indicating a stabilising effect via ionic interaction (Gasymov and Glasgow 2007).

From the ThT fluorescence binding data, it is clear that induction of amyloid properties in CBC is an exclusive property of time and concentration of MG. ThT is an amyloid reporter which, when bound to amyloid fibrils, exhibits

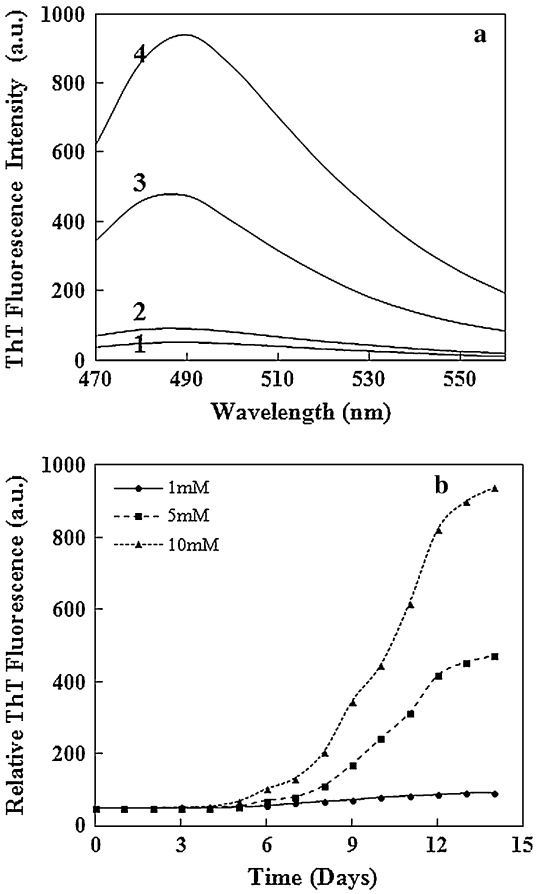

Fig. 6 **a** Thioflavin T (ThT) assay depicting the formation of fibril-like aggregates. ThT fluorescence emission spectra of native CBC (*curve 1*), *curves 2–4* show the ThT spectra of 1, 5 and 10 mM MG incubated with purified native CBC. **b** Relative ThT fluorescence of CBC incubated with different concentrations of MG for a period starting from days 0 to 14. Samples were excited at 450 nm and the emission spectra were recorded from 470 to 560 nm. Concentration of the samples was 2.5 μM and the path length was 1 cm

an enhancement in the fluorescence intensity with an emission peak at 485 nm. Figure 6 shows a typical evolution of ThT fluorescence spectra as a function of time and concentration indicating the formation of amyloid-like aggregates.

The enhancement in the fluorescence intensity of ThT upon binding to ordered protein aggregates is a rapid and sensitive method to show the presence of fibrils. Changes in fluorescence emission of ThT were monitored at regular time intervals for the incubated samples. However, maximum change has occurred at day 12–14 with maximum increase in CBC+10 mM MG incubated sample indicating rapid growth of amyloid-like aggregates. At day 14, CBC+1 mM MG incubated sample showed no such significant change in the intensity suggesting either very lengthy phase or concentration effect. This dramatic increase in fluorescence is probably due to binding of ThT to β-sheet-rich

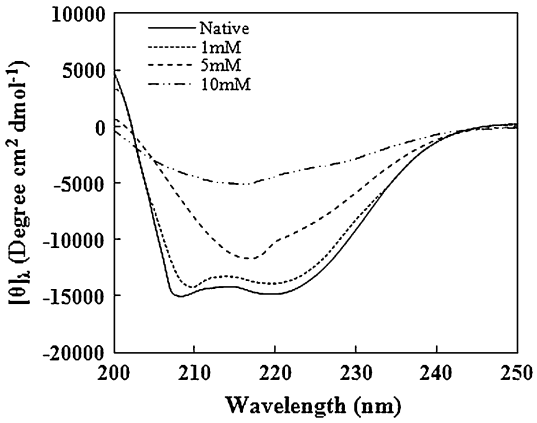

Fig. 7 Far-UV CD spectra of native and modified CBC by MG with different concentrations, in sodium phosphate buffer (50 mM, pH 7.4), 1 mM EDTA and 0.1 mM sodium azide which were incubated at 37 °C for 14 days. The *graph curves* show a decrease in the order of mean residue ellipticity (deg cm^2 mol^{-1}). Far-UV CD spectra were measured from 200 to 250 nm

deposits, which has been further confirmed by CD and FTIR studies.

Secondary structure determination

To gain insight into the structural protein modifications of CBC upon formation of amyloid-like aggregates, CD, FTIR, and Tryptophan (Trp) fluorescence spectra were recorded. As a supplement to ThT, which provides information only about the formation of fibrillar protein assemblies, far-UV CD and FTIR data reveal the overall protein secondary structural composition and their evolution to form amyloid-like aggregates.

Far-UV CD measurements were used to study the variations in protein especially α-helix to β-sheet transition. Figure 7 shows far-UV CD spectra of native CBC and incubated CBC with 1, 5, and 10 MG concentrations. The spectra in the absence of added MG show two minima one at 208 and other at 222 nm characteristic of helical structure of native CBC, which remains unmodified upon incubation. After 14 days of incubation, 10 mM MG containing protein sample no longer displayed a helical structure. Instead, the sample showed single minima at around 220 nm. The signal greatly resembles that of a β-sheet protein, in which we would expect a single minimum at around 218 nm. This indicates that high concentration conditions of MG spawn the formation of structure that is clearly less helical than the starting conformations.

Thus, the CD spectrum resembles typical spectra of proteins with high proportions of β-sheet structure, which is characterised as a consequence of the presence of amyloid-like aggregates in solution; it was also observed

upon binding with ThT. On the other hand, no significant changes in far-UV CD spectra were observed when 1 mM MG was present in the protein solution.

The secondary structural content of CBC, α-helix and β-sheet was analysed using an online tool K2D2 web server. As can be seen in Fig. 7, there is significant secondary structure change in CBC modified by MG after 14 days of incubation; the secondary structure of native CBC after 14 days of incubation was not similar to that of CBC modified by the other concentrations. After analysis, it was observed that the native CBC has a high α-helix content of 35.29 %, which started to decline by the modification of MG after 14 days of incubation reaching up to 10.34 % α-helix content of CBC modified by 10 mM MG. β-Sheet content of native CBC was found to be 17.79 % which increases gradually up to 31.24 % after 14 days of incubation by the modification of 10 mM MG. It is worth mentioning that the β-sheet structure is a prime feature of cross-linked structures of amyloid fibrils; thus, from the above data, it was suggested that the amyloid-like aggregates of CBC were formed after 14 days of incubation with MG.

FTIR studies were performed to reveal the secondary structural changes during the course of amyloid-like aggregate formation and thus validate and confirm the findings of CD spectroscopy. Protein's conformation is mostly studied in the range that constitutes the amide I band as this is the most intense absorption band for polypeptides. Amide I band of protein spans from 1,600 to 1,700 cm^{-1}, in which wave number from 1,645 to 1,662 cm^{-1} corresponds to α-helical, while β-sheet conformation corresponds to the wave number range of ~1,613–1,637 cm^{-1}, and 1,682–1,689 cm^{-1} (Damiran, and Yu 2011). Figure 8 represents the FTIR spectra of different CBC-incubated samples. FTIR spectrum of native CBC solution shows a peak at around 1,650 cm^{-1} characteristic of α-helical structure and thus indicates the presence of abundant α-helical content in native form. However, the FTIR spectrum of CBC after 12–14 days of incubation with various concentrations of MG showed a significant change in spectral properties in the amide I region. At 1 mM of MG, CBC showed somewhat less absorbance around 1,650 cm^{-1} and increased absorbance between 1,610 and 1,640 cm^{-1} as compared to native, this indicates the slight decrease in α-content and simultaneous rise in the β-sheet content. 5 mM MG caused more decrease in α-content along with further increase in β-sheet content as revealed by the shift of peak to around 1,630 cm^{-1} and emergence of a small shoulder peak at around 1,680 cm^{-1}, both of which correspond to β-sheet structures of protein. 10 mM MG showed a profound effect on the overall shape of the spectrum compared to native. The emergence of two pronounced peaks, one at 1,620 cm^{-1} and the other at 1,680 cm^{-1} signifies the abundant amyloid aggregate specific β-sheet structures induced

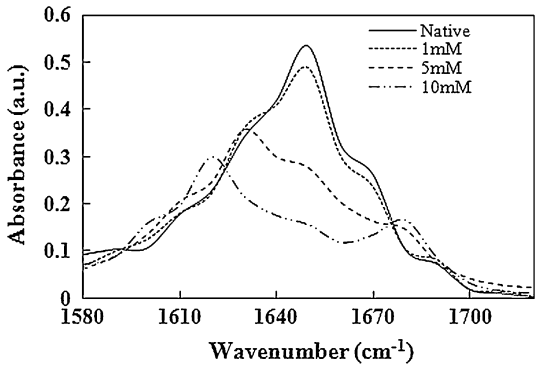

Fig. 8 FTIR spectra of the amide I region of native CBC and treated CBC with MG at different concentrations after 14 days of incubation at 37 °C

at 10 mM concentration of MG at the end of incubation period of 14 days. Shifting of the peaks in the amide I band (with lower intensity) is in agreement with previous report about the formation of amyloid fibril in case of prion protein (Jain and Udgaonkar 2010). Thus, our results clearly depict the induction of β-sheet-rich amyloid aggregates of CBC as a function of concentration of MG. This is in agreement with the CD spectra, that the aggregates possess mostly β-sheet structure thus representing the formation of β-sheet structure along with a loss in helical content upon CBC incubation with different concentrations of MG.

Microscopy analysis

The structures similar to amyloid-like aggregates of CBC formed by the modification of MG were analysed by the use of TEM. This analysis revealed that after 14 days of incubation period, bundles of fibrillar aggregates of CBC were formed. As it is clear in Fig. 9, a CBC incubated without MG did not show any type of aggregates; whereas incubation of CBC with MG for 14 days revealed direct proportionality effect of MG concentration on CBC resulting in amyloid aggregates with a length of 100–300 nm. The presence of amyloid-like aggregates in CBC is accompanied by an increase in β-sheet content as measured with CD and shown by FTIR and ThT assay; β-Sheets were not detected in solutions of CBC control.

All known amyloid fibrils, regardless of the nature of the main protein component or the source of the fibrils, are rod-like structures. In the study, fibrils display typical amyloid morphology, appear very long, straight and are approximately 100 nm. They show a distinct, twisting repeat which is similar to that observed in some preparations of Alzheimer amyloid peptides. The fibril morphology strongly suggests that the transition involves the association and winding of aggregates, possibly accompanied by a conformational change. The conformational change

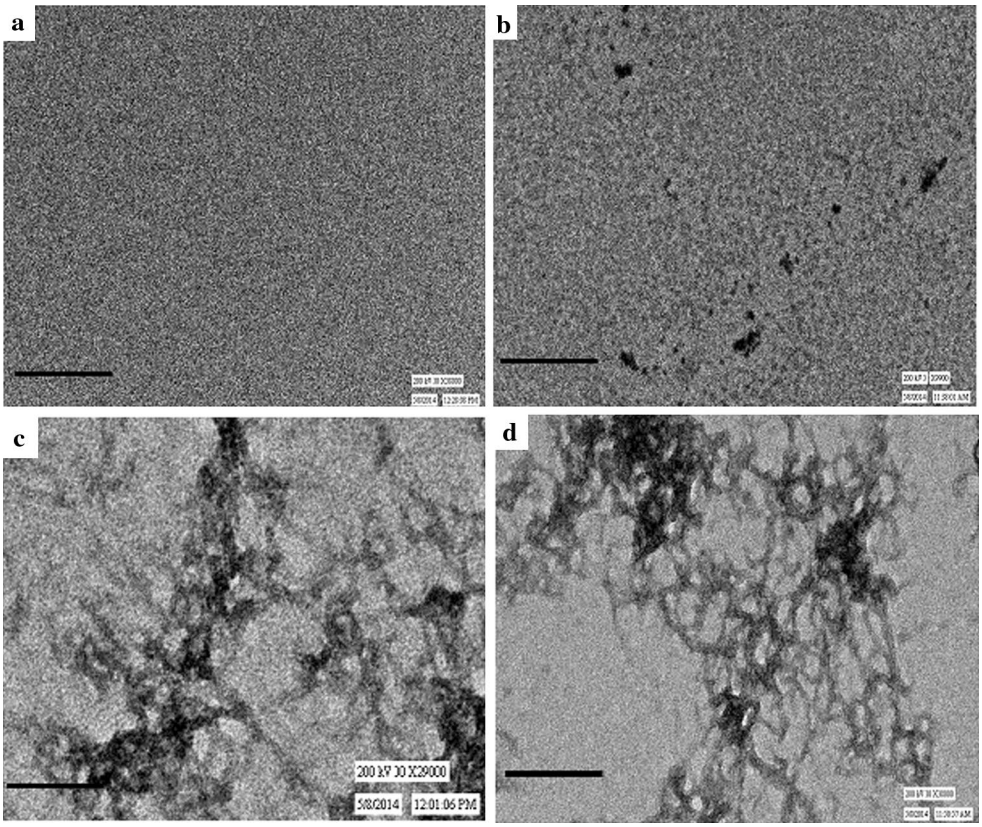

Fig. 9 Transmission electron micrographs of native and treated CBC by MG with different concentrations in sodium phosphate buffer (50 mM, pH 7.4), 1 mM EDTA and 0.1 mM sodium azide, incubated at 37 °C for 14 days showing amyloid-like aggregates. **a** Native, **b**, **c**, **d** shows 1, 5 and 10 treated CBC with MG (images were zoomed using the 100 nm *scale bar*)

scenario which is accompanied by increasing β-sheet may explain the enhanced stability of fibrils to dilution and chemical denaturation.

These results suggested that increasing concentration of MG increases the speed of polymerization of CBC into aggregates, supposed to be as a direct binding of MG with CBC and governing the change in native CBC.

Discussion

During last two decades, significant efforts have been done towards identifying, isolating and characterising the aggregate or prefibril species that are present in solution prior to the formation of fibrils, both because of their possible role in the mechanism of fibril formation and because of their implication as the toxic species involved in amyloidosis and in neurodegenerative disorders. Generally, amyloid formation arises mostly from the properties of the polypeptide chain that are similar in all peptides and proteins (Morshedi et al. 2010), but sometimes, protein misfolding results to the failure of a protein to achieve native conformation efficiently due to reduction in stability as a result of environmental change or mutation. Normally, when a polypeptide comes up from the cell or from cellular organelle, it may fold to the native state, degraded by proteolysis, or form aggregates with other molecules. Aggregation usually results in disordered species that can be degraded within the organism but it may also result in highly insoluble fibrils that accumulate in tissue. There are about twenty known diseases resulting from the formation of amyloid material including Alzheimer's, Type II diabetes, and Parkinson's disease. Amyloid fibrils are ordered protein aggregates that have an extensive beta sheet structure due to intermolecular hydrogen bonds (Selkoe 2003). The formation of the amyloid fibrils is the result of prolonged exposure to at least partially denatured conditions (Rochet and Lansbury 2000).

The present study shows that incubating the CBC with 1 mM MG could not induce any prominent structural change during this short period of incubation time, as concentration of the MG goes on increasing during this short period of incubation, CBC deviated from its native confirmation and started to unfold which ultimately lead to aggregation. Methylglyoxal may reversibly and irreversibly bind and modify proteins under physiological conditions.

This is expected to be enhanced in kidney, lens, and red blood cell proteins in diabetes mellitus, commensurate with the increase in the tissue and blood concentration of methylglyoxal (Lo et al. 1994). The assay of methylglyoxal-protein adducts in vivo is under investigation, but the involvement of methylglyoxal modification in protein in the development of diabetic complications is an interesting prospect. The formation of methylglyoxal-modified proteins in diabetes mellitus is of both prospective diagnostic importance and etiological importance in assessing glycemic control and the development of diabetic complications. Since MG is formed during glycolysis, the intracellular levels of MG are higher than circulating levels. Number of studies has used higher concentrations and doses of MG. For example, a 1 mM concentration of MG in rat pancreatic β cells caused rapid depolarization, elevated intracellular Ca^{2+} concentration and acidification in intact islets (Cook et al. 1998). MG concentration of up to 500 μM has been used to study MG-induced apoptosis of jurkat cells (Du et al. 2000). Moreover, concentration between 0.1 and 10 mM has been used to study the effect of MG on insulin-secreting cells (Sheader et al. 2001). In one in vivo study, a dose of up to 500 mg/kg MG has been used to see its effect on plasma glucose levels in cats (Jerzykowski et al. 1975). MG concentration between 2.5 and 5 mM has been used to study its effect on insulin signalling pathway in L6 muscle cells in vitro in cell culture studies (Riboulet-Chavey et al. 2006). Similar high concentrations of exogenous MG have been employed in most in vivo and in vitro studies.

Initially, the intrinsic fluorescence was done to access the interaction between MG and CBC molecule and it was observed that the MG, facilitated unfolding and generation of a possible unfolded state of CBC. This was followed by the CBC inhibitory activity assay which showed a decrease in the activity of the CBC from day 5 onwards as a result of deviation from the native conformation. This structural deviation was undoubtedly supported by the ANS fluorescence study, as the intensity of the ANS fluorescence rapidly increases suggesting the presence of unfolded state, which gets truly the bond with previous study (Fazili et al. 2014).

Unfolded regions play vital roles in promoting the aggregation of partially folded proteins. Some regions that were found to be flexible or exposed to solvent were prone to aggregation. Other regions that are not involved in the aggregation were found not to be exposed, but rather half buried even though they have high possibility of aggregating, while the exposed regions of the structure that are not involved in the aggregation have a low probability of aggregation. Proteins are in constant dynamic equilibrium so even if the folding process is complete, unfolding in the cellular environment can occur. Unfolded proteins usually refold back into their native states but if control processes fail, misfolding leads to cellular malfunctioning and consequently diseases. It has been established that failure of protein folding is a general phenomenon at elevated temperatures and under other stressful circumstances (Zervonik et al. 2006), usually proteins have the more propensity towards the interaction with other molecules being charged, possess side groups and present ubiquitously at every corner of an organism, during elevated levels of interacting molecules such as in hyperglycaemia, diabetes. Proteins/peptides come in the track and are distorted from normal/native structure. Normally, in diabetes, blood glucose level rises which form advanced glycation end products (AGEs) in different parts of the body; however, certain other molecules such as ketone bodies, glyoxal and MG have been reported which increases abnormally during different metabolic abnormalities such as obesity, type 2 diabetes, hypertension, hyperglycaemia, glucose intolerance, insulin resistance, dyslipidemia, and high blood pressure (Eckel et al. 2005).

However, decrease in the intensity of ANS fluorescence on 12–14 days could be due to the reasons of non-availability of hydrophobic residues for the dye to bind. Further, FTIR and CD confirm that the aggregated CBC mostly contains β-sheet, which is the main feature of amyloid-like aggregates. FTIR measurements displayed this fact that day 14 incubated CBC samples treated with 5 and 10 mM MG showed two amide I bands at around 1,620 and 1,680 cm^{-1}, which is possibly a cross-linked (aggregated) structure having prominent β-sheet content. Appearance of a negative ellipticity in CD analysis at 217 nm again suggests the formation of aggregated structure. Finally, ThT assay showed an increase in fluorescence intensity on day 14 compared to the native structure.

To visualise the morphology of the aggregated state of CBC, i.e. amyloid-like aggregated fibrils, TEM was employed and it was found that these fibrils are rod shaped; thus, confirming our suggestions about the formation of amyloid-like aggregates of CBC via unfolded state. Our contention that MG attributed the formation of amyloid-like aggregates of CBC is solely a concentration-dependent process, which gives the clue that type 2 diabetes, and hyperglycaemia patients are in risk of formation of protein aggregates in their bodies. Methylglyoxal is being unique because it is also produced by enzymatic processes such as glycine, threonine, and glucose catabolism. An impaired glucose fluctuation leads to a momentary elevation of triosephosphate and its degradation product, MG; this has been indirectly demonstrated by the detection of methylglyoxal-derived AGEs in the brain (Kikuchi et al. 1999). MG is believed to increase the subsequent advancement of macroangiopathy in type 2 diabetes mellitus, especially in patients who have postprandial hyperglycaemia (Rosca et al. 2002). Evidence indicates that increased MG production due to

hyperglycaemia in diabetes can impair renal mitochondrial function and lead to the development of diabetic nephropathy (DN). Moreover, it has been suggested that MG is a neurotoxic mediator of oxidative damage in the progression of AD and other neurodegenerative diseases (Lovell et al. 2001).

Thus, our study opens the door of the interaction of MG with proteins which can be a driving factor to enhance the amyloidosis.

Conclusion

The study shows that MG unfolds cystatin which may not be able to bind to cathepsins; as a result, it reduces its activity, and therefore an imbalance of protease–antiprotease occurs. Recently, it was found that binding of thiol protease inhibitor (cystatin) to Alzheimer's amyloid β inhibits in vitro amyloid fibril formation, and thus helps in preventing the progression of AD. One of the important compounds which are produced in normal and pathological conditions is MG which is at a high concentration in diabetic patients and may have a role in diabetic complexity and neurodegenerative diseases. Therefore, such study requires further attention. Also, the study is of great significance as caprine brain cystatin being a strong confederate of amyloidogenic cystatin super family and a potent endogenous regulator of cysteine proteases poses to be an attractive model to study amyloidogenesis of brain cysteine protease inhibitor.

Acknowledgments The work was supported by the project of Scientific Council of Industrial Research (CSIR) India; vide no. 37(1520)/12/EMR-II. We would like to thank All India Institute of Medical sciences, New Delhi (AIIMS) for TEM analysis, facilities available at AMU Aligarh are highly acknowledged.

Conflict of interest The authors confirm that this article content has no conflicts of interest.

References

Amin F, Khan AA, Rizvi SJ, Bano B (2011) Purification and characterization of buffalo brain cystatin. Protein Pept Lett 18:210–218

Asplund K, Hagg E, Helmers C, Lithner F, Strand T, Wester PO (1980) The natural history of stroke in diabetic patients. Acta Med Scand 207:417–424

Beisswenger BG, Delucia EM, Lapoint N, Sanford RJ, Beisswenger PJ (2005) Ketosis leads to increased methylglyoxal production on the Atkins diet. Ann N Y Acad Sci 1043(20):1–10

Bernstein HG, Kirschke H, Wiederanders B, Pollak KH, Zipress A, Rinne A (1996) The possible place of cathepsins and cystatins in the puzzle of Alzheimer disease: a review. Mol Chem Neuropathol 3:225–247

Bhat SA, Sohail A, Siddiqui AA, Bano B (2014) Effect of non-enzymatic glycation on cystatin: a spectroscopic Study. J Fluoresc 24:1107–1117. doi:10.1007/s10895-014-13-91-2

Candiloros H, Muller S, Zeghari N, Donner M, Drouin P, Ziegler O (1995) Decreased erythrocyte membrane fluidity in poorly controlled IDDM. Influence of ketone bodies. Diabetes Care 18:549–551

Carrotta R, Bauer R, Waninge R, Rischel C (2001) Conformational characterization of oligomeric intermediates and aggregates in β-lactoglobulin heat aggregation. Prot Sci 10:1312–1318

Cook LJ, Davies J, Yates AP, Elliott AC, Lovell J, Joule JA, Pemberton P, Thornalley PJ, Best L (1998) Effects of methylglyoxal on rat pancreatic beta-cells. Biochem Pharmacol 55:1361–1367

Coussons PJ, Jacoby J, McKay A, Kelly SM, Price NC, Hunt JV (1997) Glucose modification of human serum albumin: a structural study. Free Radic Biol Med 22:1217–1227

Damiran D, Yu P (2011) Molecular basis of structural makeup of hulless barley in relation to rumen degradation kinetics and intestinal availability in dairy cattle: a novel approach. J Dairy Sci 94:5151–5159

Du J, Suzuki H, Nagase F, Akhand AA, Yokoyama T, Miyata T, Kurokawa K, Nakashima I (2000) Methylglyoxal induces apoptosis in Jurkat leukemia T cells by activating c-jun N-terminal kinase. J Cell Biochem 77:333–344

Eckel RH, Grundy SM, Zimmet PZ (2005) The metabolic syndrome. Lancet 365:1415–1428

Ekiel I, Abhrahamson M (1996) Folding-related dimerization of human cystatin C. J Biol Chem 271:1314–1321

Fandrich M, Fletcher MA, Doboson CM (2001) Amyloid fibrils from muscle myoglobin. Nature 10:165–166

Fazili NA, Bhat WF, Naeem A (2014) Induction of amyloidogenicity in wild type HEWL by a dialdehyde: analysis involving multi dimensional approach. Int J Biol Macromol 64:36–44

Gasymov OK, Glasgow BJ (2007) ANS fluorescence: potential to augment the identification of the external binding sites of proteins. Biochimica Biophysica Acta 1774:403–411

Holm NK, Jespersen SK, Thomssen LV, Wolff TY, Sehgal P, Thomsen LA, Christiansen G, Andersen CB, Knudsen AD, Otzen DE (2007) Aggregation and fibrillation of bovine serum albumin. Biochim Biophys Acta 1774:1128–1138

Ii K, Ito H, Kominami E, Hirano A (1993) Abnormal distribution of cathepsin proteinases and endogenous inhibitors cystatins) in the hippocampus of patients with Alzheimer's disease, parkinsonism-dementia complex on Guam, and senile dementia and in the aged. Virchows Arch A Pathol Anat Histopathol 423:185–194

Jain S, Udgaonkar JB (2010) Salt-induced modulation of the pathway of amyloid fibril formation by the mouse prion protein. Biochemistry 49:7615–7624

Jerzykowski T, Matuszewski W, Tarnawski R, Winter R, Herman ZS, Sokola A (1975) Changes of certain pharmacological and biochemical indices in acute methylglyoxal poisoning. Arch Immunol Ther Exp (Warsz) 23:549–560

Kikuchi S, Shinpo K, Moriwaka F, Makita Z, Miyata T, Tashiro K (1999) Neurotoxicity of methylglyoxal and 3-deoxyglucosone on cultured cortical neurons: synergism between glycation and oxidative stress, possibly involved in neurodegenerative disease. J Neurosci Res 57:280–289

Kumar S, Udgaonkar JB (2009) Structurally distinct amyloid protofibrils form on separate pathways of aggregation of a small protein. Biochemistry 48:6441–6449

Kunitz M (1947) Crystalline soybean trypsin inhibitors :II General properties. J Gen Physiol 30:291–310

Laffel L (1999) Ketone bodies: a review of physiology, pathophysiology and application of monitoring to diabetes. Diabetes Metab Res Rev 15:412–426

Ledesma MD, Bonay P, Colaço C, Avila J (1994) Analysis of microtubule-associated protein tau glycation in paired helical filaments. J Biol Chem 269:21614–21619

Lo TW, Westwood ME, McLellan AC, Selwood T, Thornalley PJ (1994) Binding and modification of proteins by methylglyoxal

under physiological conditions. A kinetic and mechanistic study with *N* alpha-acetylarginine, *N* alpha-acetylcysteine, and *N* alpha-acetyllysine, and bovine serum albumin. J Biol Chem 269:32299–32305

Lovell MA, Xie C, Markesbery WR (2001) Acrolein is increased in Alzheimer's disease brain and is toxic to primary hippocampal cultures. Neurobiol Aging 22:187–194

Lowry OH, Rosebrough NJ, Farr AL, Randall RJ (1951) Protein measurement with the Folin phenol reagent. J Biol Chem 193:265–270

Marks V (1992) Recognition and differential diagnosis of spontaneous hypoglycaemia. Clin Endocrinol (Oxf) 37:309–316

McLellan AC, Thornalley PJ, Benn J, Sonksen PH (1994) Glyoxalase system in clinical diabetes mellitus and correlation with diabetic complications. Clin Sci (Lond) 87:21–29

Morshedi D, Ebrahim-Habibi A, Moosavi-Movahedi AA, Nemat-Gorgani M (2010) Chemical modification of lysine residues in lysozyme may dramatically influence its amyloid fibrillation. Biohim Biophys Acta 1804:714–722

Mussap M, Plebani M (2004) Biochemistry and clinical role of human cystatin C. Crit Rev Clin Lab Sci 41:467–550

Pulsinelli WA, Levy DE, Sigsbee B, Scherer P, Plum F (1983) Increased damage after ischemic stroke in patients with hyperglycemia with or without established diabetes mellitus. Am J Med 74:540–544

Riboulet-Chavey A, Pierron A, Durand I, Murdaca J, Giudicelli J, Van Obberghen E (2006) Methylglyoxal impairs the insulin signaling pathways independently of the formation of intracellular reactive oxygen species. Diabetes 55:1289–1299

Riddle MC, Hart J (1982) Hyperglycemia, recognized and unrecognized, as a risk factor for stroke and transient ischemic attacks. Stroke 13:356–359

Rochet JC, Lansbury PT (2000) Amyloid fibrillogenesis: themes and variations. J Curr Opin Struct Biol 10:60–68

Rosca MG, Monnier VM, Szweda LI, Weiss MF (2002) Alterations in renal mitochondrial respiration in response to the reactive oxoaldehyde methylglyoxal. Am J Physiol Ren Physiol 283:F52–F59

Sastre M, Calero M, Pawlik M, Mathews PM, Kumar A, Danilov V, Schmidt SD, Nixon RA, Frangione B, Levy E (2004) Binding of cystatin C to Alzheimer's amyloid beta inhibits in vitro amyloid fibril formation. Neurobiol Aging 8:1033–1043

Selkoe DJ (2003) Folding proteins in fatal ways. Nature 426:900–904

Semisotnov GV, Rodionova NA, Kutyshenko VP, Ebert B, Blanck J, Ptitsyn OB (1987) Sequential mechanism of refolding of carbonic anhydrase B. FEBS Lett 224:9–13

Sheader EA, Benson RS, Best L (2001) Cytotoxic action of methylglyoxal on insulin secreting cells. Biochem Pharmacol 61:1381–1386

Shinohara M, Thornalley PJ, Giardino I, Beisswenger P, Thorpe SR, Onorato J, Brownlee M (1998) Overexpression of glyoxalase-I in bovine endothelial cells inhibits intracellular advanced glycation endproduct formation and prevents hyperglycemia-induced increases in macromolecular endocytosis. J Clin Invest 101:1142–1147

Skerget K, Vifan A, Pompe-novak Turk V, Waltho JP, Tirk D, Zerovink E (2009) The mechanism of amyloid-fibril formation by stefin B: temperature and protein concentration dependence of the rates. Proteins 74:425–436

Stefani M, Dobson CM (2003) Protein aggregation and aggregate toxicity: new insights into protein folding, misfolding diseases and biological evolution. J Mol Med 81:678–699

Stephan AK, Martin CH, Janaky C, Ellen K, Maj-Linda S, David TW, Matthias S, Efrat L, Anders G, Mathias J (2007) Cystatin C modulates cerebral β-amyloidosis. Nat Genet 39:1437–1439. doi:10.1038/ng.2007.23

Stephens JM, Sulway MJ, Watkins PJ (1971) Relationship of blood acetoacetate and 3-hydroxybutyrate in diabetes. Diabetes 20:485–489

Thornalley PJ (1996) Pharmacology of methylglyoxal: formation, modification of proteins and nucleic acids, and enzymatic detoxification-a role in pathogenesis and antiprollifferative chemotherapy. Gen Pharmacol 27:565–573

Thornalley PJ, Hooper NI, Jennings PE, Florkowski CM, Jones AF, Lunec J, Barnett AH (1989) The human red blood cell glyoxalase system in diabetes mellitus. Diabetes Res Clin Pract 7:115–120

Tokunaga Y, Sakakibara Y, Kamada Y, Watanabe K, Sugimot Y (2013) Analysis of core region from egg white lysozyme forming amyloid fibrils. Int J Biol Sci 9:219–227

Turk V, Stoka V, Turk D (2008) Cystatins: biochemical and structural properties, and medical relevance. Front bioscience 13:5406–5420

Uversky VN, Li J, Fink AL (2001) Evidence for a partially folded intermediate in alpha-synuclein fibril formation. J Biol Chem 276:10737–10744

Wang X, Desai K, Clausen JT, Wu L (2004) Increased methylglyoxal and advanced glycation end products in kidney from spontaneously hypertensive rats. Kidney Int 66:2315–2321

Wang X, Chang T, Jiang B, Desai K, Wu L (2007) Attenuation of hypertension development by aminoguanidine in spontaneously hypertensive rats: role of methylglyoxal. Am J Hypertens 20:629–636

Zerovnik E, Skarabot M, Skerget K, Giannini S, Stoka V, Jenko-Kokalj S, Staniforth RA (2007) Amyloid fibril formation by human stefin B: influence of pH and TFE on fibril growth and morphology. Amyloid 3:237–247

Zervonik E, Skerget K, Tusi- Znidaric M, Loeschner C, Brazier MW, Brown DR (2006) High affinity copper binding by stefin B (cystatin B) and its role in the inhibition of amyloid fibrillation. FEBS J 273:4250–4263